



# University of HUDDERSFIELD

## University of Huddersfield Repository

Abuaniza, Ayman, Fletcher, Simon and Longstaff, Andrew P.

Thermal error modelling of a three axes vertical milling machine using Finite element analysis (FEA)

### Original Citation

Abuaniza, Ayman, Fletcher, Simon and Longstaff, Andrew P. (2013) Thermal error modelling of a three axes vertical milling machine using Finite element analysis (FEA). In: Proceedings of Computing and Engineering Annual Researchers' Conference 2013 : CEARC'13. University of Huddersfield, Huddersfield, pp. 87-92. ISBN 9781862181212

This version is available at <http://eprints.hud.ac.uk/id/eprint/19369/>

The University Repository is a digital collection of the research output of the University, available on Open Access. Copyright and Moral Rights for the items on this site are retained by the individual author and/or other copyright owners. Users may access full items free of charge; copies of full text items generally can be reproduced, displayed or performed and given to third parties in any format or medium for personal research or study, educational or not-for-profit purposes without prior permission or charge, provided:

- The authors, title and full bibliographic details is credited in any copy;
- A hyperlink and/or URL is included for the original metadata page; and
- The content is not changed in any way.

For more information, including our policy and submission procedure, please contact the Repository Team at: [E.mailbox@hud.ac.uk](mailto:E.mailbox@hud.ac.uk).

<http://eprints.hud.ac.uk/>

## Thermal error modelling of a three axes vertical milling machine using Finite element analysis (FEA)

Ayman A. Abuaniza, Simon Fletcher, Andrew P. Longstaff  
University of Huddersfield, Queensgate, Huddersfield HD1 3DH, UK

### ABSTRACT

Thermal errors in machine tools have a detrimental effect on the accuracy of components they produce. In order to reduce the influence of thermal errors, the propagation of heat through the structure of the machine needs to be understood. The modelling of thermal error of small three axes vertical milling centre (VMC) machine tools is introduced in this paper. Firstly, a thermal imaging camera and non-contact displacement transducer (NCDT) sensors were used to measure the temperature and thermal deformation in X, Y, Z axes respectively during spindle heating and cooling cycles. Secondly, a model of the VMC was created using SolidWorks software and simulated using finite element analysis (FEA). The boundary conditions are calculated according to measured parameters like, temperatures of machine structure, heat transfer coefficients and ambient temperature. Of particular importance is the heat power of heat generating components in the machine such as the main spindle motor and bearings. These parameters vary with machine use and are calculated using energy balance calculations and thermal imaging data. Finally, the FEA simulated results are obtained and are in close correlation with the experimental results. Such accurate FEA simulations permit offline assessments to be made of temperature gradients and displacements in machine tools structures, reducing the need for expensive on-line testing. Furthermore, correlation coefficient analysis is employed to validate the simulated model temperature; the thermal error was reduced up to 90%, from 35  $\mu\text{m}$  to within 4  $\mu\text{m}$ . Therefore, the VMC thermal error is minimised and component accuracy improved.

Keywords: Finite element analysis (FEA), thermal errors, displacement, temperature gradient.

### INTRODUCTION

Temperature changes in machine tool structures occur as a result of two reasons; firstly internal heat sources like belt drives, motors and bearings and secondly from external heat sources such ambient temperature change of the workshop. These changes in the temperature of the machine tools structure causes non-linear deformation of the structural elements and results in displacement of the cutting tools relative to the work piece and is commonly known as thermal error. Thermal errors have been reported to account for around 70% of the total volumetric error [1].

There are generally three ways for reducing the thermal error, they are

- 1) *Avoidance of thermal error.* Thermal errors can be minimized through improvements in machine design including the use of symmetry and low expansion coefficient of materials [2].
- 2) *Control of thermal error.* Temperature of all machine tool elements has to remain stable using cooling systems or heat pipes [3].
- 3) *Thermal error compensation.* This way plans to electronically compensate dimensional error caused by thermal variation typically using a model and temperature information [4].

The first and the second methods can reduce the thermal errors effectively. However, avoidance and control of thermal error can usually only be implemented during machine tool design and construction phases and may add significant cost. Compensation of thermal error can be easy to apply and relatively economical, as its principle is simple. Spindles and other high speed rotating parts in machine tools are often the most significant heat sources and contribute significantly to the total error. Prior to the compensation process, the thermal error needs to be modelled.

Modelling of the thermal error can be a convenient and cost-effective method for minimising machine tool thermal error and therefore attracts the attention of many researchers around the world. Finite element analysis has been used widely in modelling of the thermal error of machine tools. Haitao, Z., et al [5] used FEA to simulate the temperature and the thermal error of the spindle of a CNC machine tool. The results showed that the simulation data agreed well (approximately 95%) with the

experimental results. Creighton & et al [6] did an experiment on a machine tool to record the temperature and thermal deformation of the spindle at different rotational speeds using thermal resistance temperature sensors and capacitive displacement sensors. Then the spindle thermal error model was built by FEA based on the experimental data. They concluded that FEA results match well with the experimental data which indicates that a simple compensation scheme can be applied in industrial workshop without big investment of time, material and manpower.

Most studies concentrated on the thermal deformation simulation of the main spindle system only and lacked reliable whole-machine simulation models. Consequently, such studies can reveal the thermal deformation process of the spindle system to a certain extent but cannot give a true image of the actual situation of the whole-machine thermal deformation.

This paper aims to introduce an effective and simple method to model the whole structure of a small VMC and simulate the thermal error. Initially a thermal imaging camera and non-contact displacement transducers (NCDTs) are used to obtain the temperature data and the spindle thermal deformation in X Y and Z axes at different working conditions. These tests are designed to be short to minimise down-time on the machine but maximise data for the calculation of the boundary conditions. Secondly, the finite element analysis FEA was carried out to predict the temperature gradient and thermal deformation of the small VMC. The accuracy of the simulation analysis was increased by setting boundary conditions according to the measured parameters like machine structure temperatures, ambient temperature and so on.

### EXPERIMENTAL TEST AND ESTABLISHMENT OF THERMAL ERROR MODEL

During the experiment a Flir ThermaCAM S65 thermal imaging camera, which has a stated accuracy of  $\pm 2^{\circ}\text{C}$ , was used to monitor the heat flow through the machine structure while the spindle rotates at 8000 rpm (close to its maximum speed) for two hours heating and stopped one hour for cool down. The location was chosen so that the heat flow into the spindle, head slide and motor can be monitored. The accuracy of the thermal image was improved by applying masking tape (with identified emissivity of (0.95) to areas of thermal interest and averaging the images to decrease noise [7]. Figure 1 shows the thermal image camera set up and a thermal image at the end of heating up period. Eddy current NCDTs measurement sensors were used to measure the spindle deformation in X, Y and Z axes. The set-up of the NCDTs is shown in Figure 2.

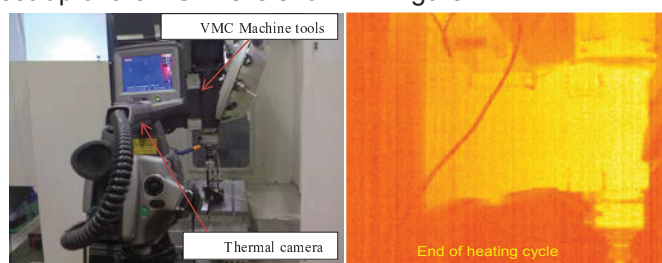


Figure 1 Thermal image camera set up and a thermal image

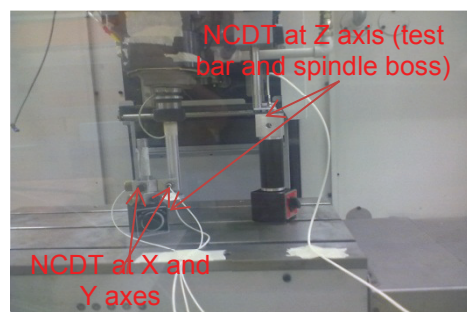


Figure 2 NCDT sensors set up

### FINITE ELEMENT ANALYSIS (FEA)

The FEA was carried out using Dassault Systemes Simulation (Part of the Solidworks suite of software) to predict the temperature gradient and the spindle thermal deformation. In order to

minimise the time of calculation, the geometric model of the VMC is simplified to shorten the computation time for finite-element simulation. This simplification includes elimination of small holes, curvature, chamfers, bolts and bolt holes. See Figure 3. The lower spindle bearing, upper spindle bearing and motor are considered to be internal heat sources. The lower and upper bearings are angular contact ball bearings as they are loaded both axially and radially. They are located close to the spindle nose and the top of the spindle system respectively. Modelling the full machine was used to match the long term industrial operating conditions.

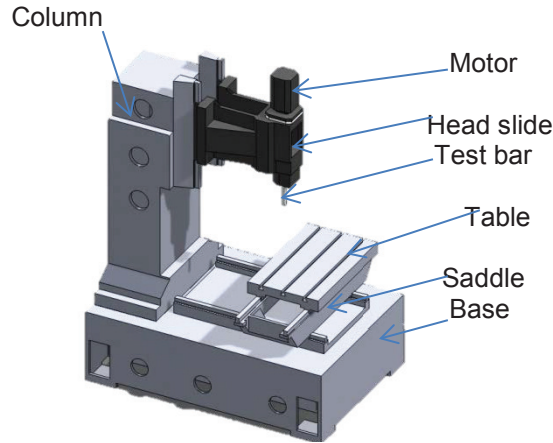


Figure 3 Simplified geometrical model of VMC

The model was meshed using the curvature mesh method. High density mesh was applied to structures adjacent to heat sources only resulting in a total of 41369 elements. Elements size is determined considering both the time of calculation and the simulation accuracy. The spindle and associated rotational components are made of steel, the test bar from Aluminium and the structure from grey cast iron. Table 1 shows the applied material properties. For the various joints where components are bolted together, the effect of thermal contact resistance was applied. Its value is  $0.0004 \text{ m}^2 \cdot \text{°C}/\text{W}$  explained by Mian [8].

Table 1 material properties

Material	Grey cast iron	steel	Aluminium
Density $\text{Kg}/\text{m}^3$	7200	7800	2700
Modulus of elasticity (Pa)	$6.61 \cdot 10^{10}$	$2 \cdot 10^{11}$	$7.2 \cdot 10^{10}$
Poisson's ratio	0.27	0.32	0.33
Specific heat $(\frac{\text{j}}{\text{kg} \cdot \text{°C}})$	510	500	960
Thermal conductivity (W/m.k)	45	30	120
Thermal expansion coefficient (1/°C)	$1.2 \cdot 10^{-5}$	$1.2 \cdot 10^{-5}$	$2.5 \cdot 10^{-5}$

The thermal load of bearings and spindle motor are calculated using equation (1) applied to specific parts of the structure. The equation parameters: the VMC structure temperature, the ambient temperature and area, are obtained from experiments and then the heat power and boundary conditions are computed on the basis of those experimental data and applied to the model. A convective coefficient of  $92 (\frac{\text{W}}{\text{m}^2 \cdot \text{°C}})$  was applied to exposed rotating parts such as the test bar when the spindle is active and a value of  $6 (\frac{\text{W}}{\text{m}^2 \cdot \text{°C}})$  applied while the spindle is stopped and to the rest of VMC surfaces. In order to determine the magnitude of the heat generated by the complex heat sources such as bearings, an efficient energy balance method, explained by Mian et al [9], is employed. Using thermal imaging to monitor the flow of temperature and equation 1, the energy input into part of the structure over time can be estimated and used in the FEA. Figure 4 shows nonlinear relationship of the lower spindle bearing heat power.

$$Q = (mc_p(T_2 - T_1))/t + hA(T_{\text{surface}} - T_{\text{air}}) \dots \dots \dots (1)$$

Where Q heat rate (W), m mass (kg),  $c_p$  specific heat  $(\frac{\text{j}}{\text{kg} \cdot \text{°C}})$ ,  $(T_2 - T_1)$  temperature change(°C), t time (s), h coefficient of convection  $(\frac{\text{W}}{\text{m}^2 \cdot \text{°C}})$ ,  $T_{\text{surface}}$  surface temperature (°C),  $T_{\text{air}}$  . ambient temperature(°C)

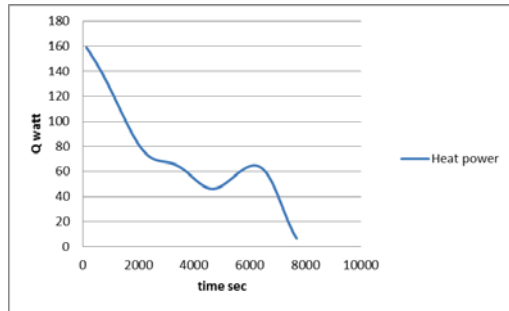


Figure 4 lower spindle bearing heat power

**TEMPERATURE AND DISPLACEMENT SIMULATIONS.**

The simulation time was the same as for the experiment: 2 hours spindle heating and 1 hour cooling down. Figure 5 shows the simulated temperature gradient in the VMC assembly and the simulated machine behaviour as a result of thermal distribution. Temperature and deformation results were taken from the nodes located at similar place to the actual thermal image spot locations on the machine (temperature and NCDTs).

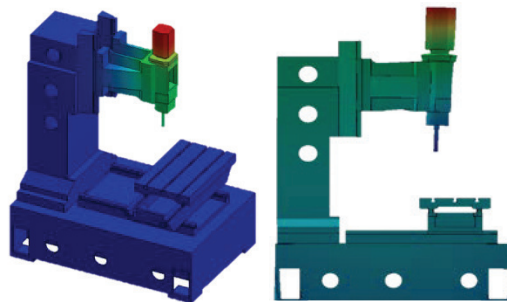


Figure 5 VMC simulated model. Temperature (left) and distortion (right)

**CORRELATION COEFFICIENT**

Correlation coefficient is one of the standard statistical coefficients. It signifies the closeness of two arbitrary variables (X and Y) and its formula is showed as follows.

$$r = \frac{\sum_{i=1}^n ((x_i - \bar{x})(y_i - \bar{y}))}{\sqrt{\sum_{i=1}^n (x_i - \bar{x})^2 \sum_{i=1}^n (y_i - \bar{y})^2}} \quad \dots (2)$$

Where x and y are the experimental values of temperature or displacement and y the simulated values respectively.

As r approaches 1, it indicates that the two variables increasingly relate to each other [10]. Based on thermal imaging camera data and simulation results of the VMC model, correlation coefficients of experiment and simulated data calculated at places close to the heat sources and VMC axes are more than 90%. See Figure 6 and Figure 7.

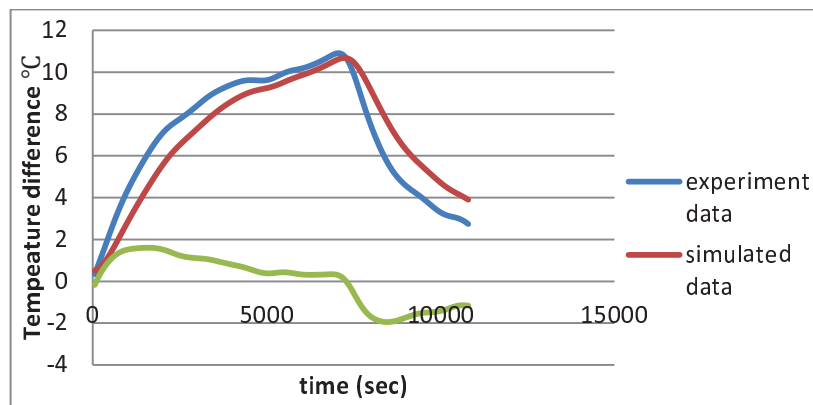


Figure 6 Experiment and simulated temperature at spindle nose

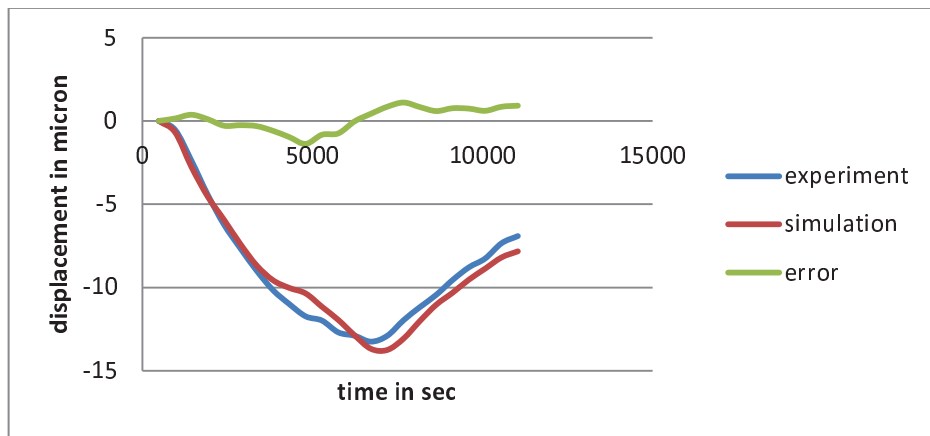


Figure (7) displacement in Z axis

Furthermore, the temperature of various parts on the side of the carrier (from thermal imaging) was correlated with the same carrier surface on the model as indicated in Figure 8. The correlation coefficient of selected spots, area and axes displacement is indicated in table 2 and table 3.

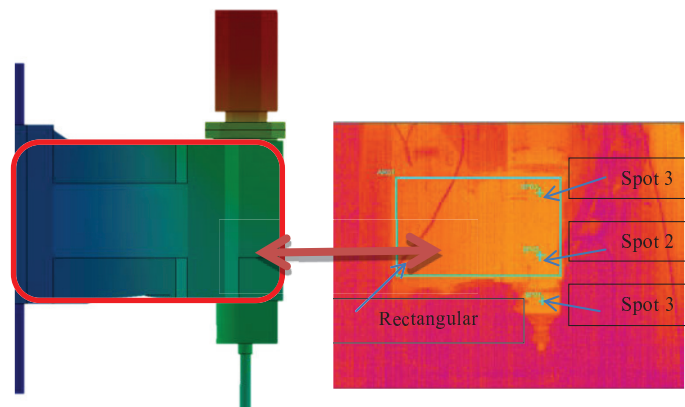


Figure 8 The selected area on the head slide model and thermal image

Table 2 Correlation coefficient at points of interest

Places on the carrier	Spot 1	Spot 2	Spot 3	The rectangle
Correlation Coefficient	0.92	0.91	0.91	0.90

Table 3 Axes displacement correlation coefficient

VMC Axes	X axis	Y axis	Z axis
Correlation Coefficient	0.97	0.98	0.98

It is clear from the correlation coefficient values that the experiment and simulated results are close to each other. An additional comparison was made using measurement of temperature over an area of the surface, not just at a specific point. This will help indicate total energy input. An average temperature of the rectangle shown in Figure 8 taken from the thermal camera images was compared with the same area of the surface model temperature nodes. The result in Figure 9 shows they correlate by (91%).

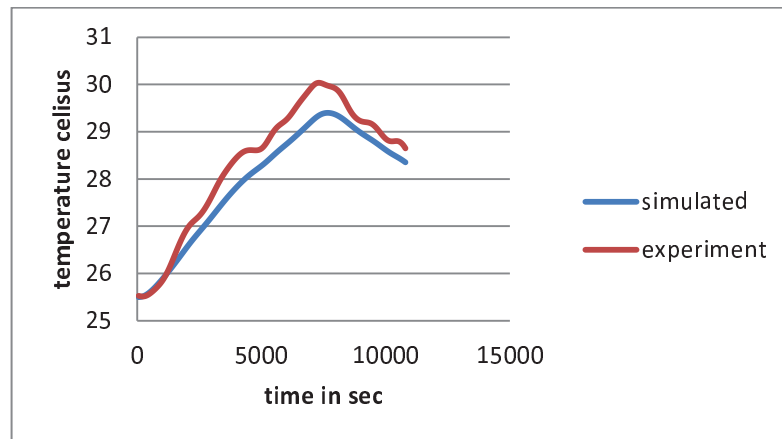


Figure 9 head slide side temperature correlation

### CONCLUSIONS

This paper presents an FEA based method of predicting the thermal errors in a small VMC. Experimental work was conducted to obtain the thermal behaviour of the machine structure by running the main spindle and recording temperature gradient and displacement data. The predicted temperature rise and displacement data from the simulations fit the experimental data well. The correlation coefficient was calculated at points of thermal interest to obtain the closeness between the experiment and simulated data which was calculated to be more than 90%. The accurate simulations can be used to predict errors under different operating conditions and to develop compensation models. Thermal error could be reduced to just 4  $\mu\text{m}$  in the Z and Y axis directions from 35 and 20  $\mu\text{m}$  respectively. The error in the X axis is negligible on this configuration of machine due to structural symmetry.

### REFERENCES

1. Bryan, J., *International status of thermal error research*, . Annals of the CIRP, 1990. **vol 39**( number 2): p. pp 573-645.
2. Ramesh, R., *Error compensation in machine tools — a review Part II: thermal errors*. International Journal of Machine Tools and Manufacture, 2000. **40**(9): p. 1257-1284.
3. Weck, M., et al., *Reduction and Compensation of Thermal Errors in Machine Tools*. CIRP Annals - Manufacturing Technology, 1995. **44**(2): p. pp 589-598.
4. Yang, S., J. Yuan, and J. Ni, *Accuracy enhancement of a horizontal machining center by real-time error compensation*. Journal of Manufacturing Systems, 1996. **15**(2): p. 113-124.
5. Haitao, Z., Y. Jianguo, and S. Jinhua, *Simulation of thermal behavior of a CNC machine tool spindle*. International Journal of Machine Tools and Manufacture, 2007. **47**(6): p. pp 1003-1010.
6. Creighton, E., et al., *Analysis of thermal errors in a high-speed micro-milling spindle*. International Journal of Machine Tools and Manufacture, 2010. **50**(4): p. pp 386-393.
7. Fletcher, S., A.P. Longstaff, and A. Mayers, *Measurement methods for efficient thermal assessment and error-compensation*. Proceedings of the Topical Meeting: Thermal Effects in Precision Systems – Maastricht., 2007.
8. Mian, N.S., et al., *Efficient Offline Thermal Modelling for Accurate Assessment of Machine Tool Thermal Behaviour*. 2009.
9. Mian, N.S., et al., *Efficient thermal error prediction in a machine tool using finite element analysis*. MEASUREMENT SCIENCE AND TECHNOLOGY, 2011. **22**(8): p. pp 85-107.
10. Yang, L. and Z. Wanhua. *Axial thermal error compensation method for the spindle of a precision horizontal machining center*. IEEE.